

Bayesian Markov Switching Tensor Regression for Time-varying Networks

Monica Billio*

Department of Economics, Ca' Foscari University of Venice
and

Roberto Casarin

Department of Economics, Ca' Foscari University of Venice
and

Matteo Iacopini

Scuola Normale Superiore of Pisa

July 5, 2019

Abstract

We propose a new Bayesian Markov switching regression model for multidimensional arrays (tensors) of binary time series. We assume a zero-inflated logit regression with time-varying parameters and apply it to multilayer temporal networks. The original contribution is threefold. First, to avoid over-fitting we propose a parsimonious parametrization based on a low-rank decomposition of the tensor of regression coefficients. Second, we assume the parameters are driven by a hidden Markov chain, thus allowing for structural changes in the network topology. We follow a Bayesian

*We are grateful to Federico Bassetti, Sylvia Frühwirth-Schnatter, Christian Gouriéroux, Alain Monfort and Christian Robert for their comments and suggestions on earlier versions of this paper. Also, we thank the seminar participants in CREST. Moreover, we thank the conference and workshop participants at: “12th CFENetwork” in Pisa, 2018, “DYSES” in Paris, 2018, “46th SSC” in Montréal, 2018, “1st QFFE” in Marseille, 2018, “8th MAF” in Madrid, 2018, “11th CFENetwork” in London, 2017, “8th ESOBE” in Maastricht, 2017, “1st Italian-French Statistics Seminar” in Venice, 2017, “41st AMASES” in Cagliari, 2017 and “1st EcoSta” in Hong Kong, 2017. This work was supported by the Université Franco-Italienne under Grant “Bando Vinci 2016”. This research used the SCSCF multiprocessor cluster system at Ca' Foscari University of Venice.

approach to inference and provide an efficient Gibbs sampler for posterior approximation. We apply the methodology to a real dataset of financial networks to study the impact of several risk factors on the edge probability. Supplementary materials for this article are available online.

Keywords: multidimensional data; sparsity; nonlinear time series; zero-inflated logit

1 Introduction

The analysis of large sets of binary data is a central issue in many fields such as biostatistics ([45], [54]), image processing ([56]), machine learning ([4], [34]), medicine ([16]), text analysis ([50]) and statistics ([44], [46], [52]).

In this paper we consider binary series representing the edge activation in time-varying ([29]) and multilayer networks ([8]). The application focuses on financial networks since, in spite of the wide literature on theoretical models (e.g. [1], [13], [40], [24]), the statistical analysis of their dynamical properties is still at its infancy (e.g., [7] and [19]). The study of temporal networks is very interdisciplinary and we expect our statistical framework to be of interest for many disciplines.

The first issue in building a dynamic network model concerns the impact of covariates on the dynamic process of link formation. We propose a parsimonious model that can be successfully used to this aim, relying on tensors and their decompositions. See [36], [18] and [17] for a review. The main advantage in using tensors is the possibility of dealing with the complexity of novel data structures which are becoming increasingly available, such as networks, multilayer networks, three-way tables, spatial panels with multiple series observed for each unit (e.g., municipalities, regions, countries). The use of tensor algebra has the advantage of preventing data reshape and manipulation, and preserving data intrinsic structure. Another advantage of tensors stems from the decompositions and approximations, which provide representations in lower dimensional spaces (see ch.7-8 of [27]). In this paper, we exploit the parallel factor (PARAFAC) decomposition for reducing the number of parameters to estimate, thus making inference on network models feasible.

Another issue in network modelling regards the time variation of the network topology. For example, structural breaks have been detected by [7], [2] and [6] in contagion networks and [23] found evidence of link persistence in interbank networks. Starting from these stylized facts, we propose a new Markov switching model for capturing structural changes in

temporal networks. After [28], the Markov switching dynamics has been used in several time series models, such as VARs ([47]), factor models ([32]), dynamic panels ([31]), stochastic volatility ([15]), ARCH and GARCH ([26]) and stochastic correlation ([12]). See [22] for an introduction to Markov switching models. We contribute to this literature by applying Markov switching to tensor valued data.

Many real world temporal networks exhibit sparsity ([42]) and sudden abrupt changes in the sparsity level across time. See also [3] for an empirical evidence on financial networks. Motivated by this observation, we propose a zero-inflated logit regression for the edge activation and allow for Markov switching sparsity levels. We contribute to the statistics literature on models for network data ([20], [53], [10], [14], [5], [48], [35]) and matrix-valued data ([55], [11]) by proposing a nonlinear model for sparse tensor-valued data.

The remainder of this paper is organized as follows. Section 2 presents the model. Sections 3-4 discuss the Bayesian inference procedure. Section 5 provides an application to financial network data. Concluding remarks are given in Section 6. Further details and results are provided in the supplementary material.

2 A Markov Switching Model for Networks

Relevant objects in our modelling framework are D -order tensors $\mathcal{X} \in \mathbb{R}^{d_1 \times \dots \times d_D}$ of size $(d_1 \times \dots \times d_D)$, that are D -dimensional arrays, elements of the tensor product of D vector spaces, each one endowed with a coordinate system. See [27] for an introduction to tensor spaces. A tensor can be thought of as the multidimensional extension of a matrix (i.e., a 2-order tensor), where each dimension is called mode. Other objects of interest in this paper are tensor slices, i.e. matrices obtained by fixing all but two of the indices of the array, and tensor fibers, i.e. vectors resulting from keeping fixed all indices but one. See Appendix A for some background material on tensors.

Tensors are particularly useful for representing multilayer temporal networks ([8] and [33]). Let $G_t = (V_1, V_2, M, E_t)$ be a multilayer temporal network, where $V_1 = \{1, \dots, I\}$, $V_2 = \{1, \dots, J\}$ are two vertex sets, $M = \{1, \dots, K\}$ is the set of layers and $E_t \subset (V_1 \times V_2 \times M)$ is the edge set at time $t = 1, \dots, T$. The network connectivity can be encoded in a 4-order tensor \mathcal{X} of size $(I \times J \times K \times T)$, with entries

$$x_{ijk,t} = \begin{cases} 1 & \text{if } \{i, j, k\} \in E_t \\ 0 & \text{if } \{i, j, k\} \notin E_t. \end{cases} \quad (1)$$

This definition is general enough to include undirected and directed networks, and undirected bipartite networks. It can be further extended to account for other types of networks ([33]). One of the most recurrent features of observed networks is sparsity. In random graph theory sparsity is defined asymptotically as the feature of a network where the number of edges grows subquadratically with the number of nodes [?, see[ch.7]Diestel12GraphTheory]. In finite graphs, sparsity occurs when there is an excess of zeros in the connectivity tensor, that is, when the degree distribution has a peak at 0.

To describe network sparsity we assume that the probability of observing an edge in each layer of the network is a mixture of a Dirac mass at 0 and a Bernoulli distribution. Since the sparsity pattern in many real networks is not time homogeneous, we assume that both the mixing and the Bernoulli probabilities are time-varying. Finally, a logistic regression is assumed to include covariates. In summary, for each entry $x_{ijk,t}$ of the tensor \mathcal{X}_t (that is, each edge of the corresponding network) we assume a zero-inflated logit regression model

$$\begin{aligned} x_{ijk,t} | \rho(t), \mathbf{g}_{ijk}(t) &\sim \rho(t) \delta_{\{0\}}(x_{ijk,t}) + (1 - \rho(t)) \delta_{\{d_{ijk,t}\}}(x_{ijk,t}) \\ d_{ijk,t} &= \mathbb{1}_{\mathbb{R}_+}(x_{ijk,t}^*) \\ x_{ijk,t}^* &= \mathbf{z}'_{ijk,t} \mathbf{g}_{ijk}(t) + \varepsilon_{ijk,t} \quad \varepsilon_{ijk,t} \stackrel{iid}{\sim} \text{Logistic}(0, 1). \end{aligned} \quad (2)$$

where $\mathbf{z}_{ijk,t} \in \mathbb{R}^Q$ is a vector of edge-specific covariates and $\mathbf{g}_{ijk}(t) \in \mathbb{R}^Q$ is a time-varying edge-specific vector of parameters and $\rho(t)$ is the time-varying probability of excess of zeros

in the network. Without loss of generality, we assume the set of covariates is common to all edges, i.e. $\mathbf{z}_{ijk,t} = \mathbf{z}_t$. The specification of the model is completed with the assumption that the parameters $\rho(t)$ and $\mathbf{g}_{ijk}(t)$ are driven by a hidden Markov chain $\{s_t\}_{t=1}^T$ with finite state space $\{1, \dots, L\}$, that is $\rho(t) = \rho_{s_t}$ and $\mathbf{g}_{ijk}(t) = \mathbf{g}_{ijk,s_t}$. The transition matrix of the chain is assumed to be time-invariant and denoted by $\Xi = (\xi'_1, \dots, \xi'_L)'$, where $\xi_l = (\xi_{l,1}, \dots, \xi_{l,L})$ is a probability vector and $\xi_{i,j} = p(s_t = j | s_{t-1} = i)$ is the transition probability from state i to state j .

By integrating out $x_{ijk,t}^*$ in eq. (2), we obtain the regime-specific probabilities of observing an edge from i to j in the layer k

$$p(x_{ijk,t} = 1 | \rho_l, \mathbf{g}_{ijk,l}) = (1 - \rho_l) \frac{\exp(\mathbf{z}'_t \mathbf{g}_{ijk,l})}{1 + \exp(\mathbf{z}'_t \mathbf{g}_{ijk,l})} \quad (3)$$

$$p(x_{ijk,t} = 0 | \rho_l, \mathbf{g}_{ijk,l}) = \rho_l + (1 - \rho_l) \left(1 - \frac{\exp(\mathbf{z}'_t \mathbf{g}_{ijk,l})}{1 + \exp(\mathbf{z}'_t \mathbf{g}_{ijk,l})} \right). \quad (4)$$

For the ease of notation, we provide a compact representation of the general model. First, we define $\mathbb{X}^d = \{\mathcal{X} \in \mathbb{R}^{i_1 \times \dots \times i_d}\}$ the set of real valued d -order tensors of size $(i_1 \times \dots \times i_d)$, $\mathbb{X}_{0,1}^d = \{\mathcal{X} \in \mathbb{R}^{i_1 \times \dots \times i_d} : \mathcal{X}_{i_1, \dots, i_d} \in \{0, 1\}\} \subset \mathbb{X}^d$ the set of adjacency tensors of size $(i_1 \times \dots \times i_d)$, and $\Psi : \mathbb{X}^d \rightarrow \mathbb{X}_{0,1}^d$ a linear operator such that $\mathcal{X}^* \mapsto \Psi(\mathcal{X}^*) \in \{0, 1\}^{i_1 \times \dots \times i_d}$. For a tensor \mathcal{X}_t^* with k -th slice $\mathbf{X}_{k,t}^* \in \mathcal{X}^{I,J}$ it is possible to write the model in tensor form by $\Psi(\mathbf{X}_{k,t}^*) = (\mathbf{1}_{\mathbb{R}_+}(x_{ijk,t}^*))_{i,j}$, where $\mathbf{1}_A(x)$ is the indicator function, which takes value 1 if $x \in A$ and 0 otherwise.

Second, we define the mode- n product between a D -order tensor $\mathcal{X} \in \mathbb{R}^{d_1 \times \dots \times d_D}$ and a vector $\mathbf{v} \in \mathbb{R}^{d_n}$, as a $(D-1)$ -order tensor $\mathcal{Y} \in \mathbb{R}^{d_1 \times \dots \times d_{n-1} \times d_{n+1} \times \dots \times d_D}$ whose entries are

$$\mathcal{Y}_{(i_1, \dots, i_{n-1}, i_{n+1}, \dots, i_D)} = (\mathcal{X} \times_n \mathbf{v})_{(i_1, \dots, i_{n-1}, i_{n+1}, \dots, i_D)} = \sum_{i_n=1}^{d_n} \mathcal{X}_{i_1, \dots, i_n, \dots, i_D} \mathbf{v}_{i_n}. \quad (5)$$

By collecting the coefficients $\mathbf{g}_{ijk}(t)$ along the indices i, j, k in a 4-order tensor $\mathcal{G}(t) \in$

$\mathbb{R}^{I \times J \times K \times Q}$, we can rewrite eq. (2) in the compact form:

$$\begin{cases} \mathcal{X}_t = \mathcal{B}(t) \odot \Psi(\mathcal{X}_t^*) & b_{ijk}(t) \stackrel{iid}{\sim} \mathcal{Bern}(1 - \rho(t)) \\ \mathcal{X}_t^* = \mathcal{G}(t) \times_4 \mathbf{z}_t + \mathcal{E}_t & \varepsilon_{ijk,t} \stackrel{iid}{\sim} \mathcal{Logistic}(0, 1) \end{cases} \quad (6)$$

where $\mathcal{B}(t) \in \{0, 1\}^{I \times J \times K}$ and $\mathcal{E}_t \in \mathbb{R}^{I \times J \times K}$ are tensors of the same size of \mathcal{X}_t , with entries $b_{ijk}(t)$ and $\varepsilon_{ijk,t}$, respectively, and the symbol \odot is the Hadamard product ([36]). Matrix operations and results from linear algebra can be generalized to tensors (see [27], [37]). This model is closely related to a switching regression representation (see Ch. 8 of [22]) which can be used to carry out inference simultaneously for all coefficient tensors. By introducing a dummy coding for s_t through L binary variables $\zeta_{t,l} = \mathbb{1}_{\{l\}}(s_t)$, $l = 1, \dots, L$, model (6) is written as

$$\begin{cases} \mathcal{X}_t = \mathcal{B}(t) \odot \Psi(\mathcal{X}_t^*) & b_{ijk}(t) \stackrel{iid}{\sim} \mathcal{Bern}(1 - \rho(t)) \\ \mathcal{X}_t^* = \mathcal{G} \times_4 (\boldsymbol{\zeta}_t \otimes \tilde{\mathbf{z}}_t)' + \mathcal{E}_t = \mathcal{G} \times_4 (\boldsymbol{\zeta}_t, \boldsymbol{\zeta}_t \otimes \mathbf{z}_t)' + \mathcal{E}_t & \varepsilon_{ijk,t} \stackrel{iid}{\sim} \mathcal{Logistic}(0, 1) \\ \boldsymbol{\zeta}_{t+1} = \Xi \boldsymbol{\zeta}_t + \tilde{\mathbf{u}}_t & \mathbb{E}[\tilde{\mathbf{u}}_t | \tilde{\mathbf{u}}_{t-1}] = 0 \end{cases} \quad (7)$$

which is a switching SUR ([57], [6]), where \otimes denotes the Kronecker product, $\{\tilde{\mathbf{u}}_t\}_t$ is a martingale difference process, $\tilde{\mathbf{z}}_t = (1, \mathbf{z}_t)'$ and $\boldsymbol{\zeta}_t = (\zeta_{t,1}, \dots, \zeta_{t,L})'$.

We propose a parsimonious parametrisation of the model by exploiting tensor representations (see [36] for a review). In particular we assume a PARAFAC decomposition with fixed rank R for the tensor $\mathcal{G}(t) = \mathcal{G}_{s_t}$:

$$\mathcal{G}(t) = \sum_{r=1}^R \boldsymbol{\gamma}_1^{(r)}(t) \circ \boldsymbol{\gamma}_2^{(r)}(t) \circ \boldsymbol{\gamma}_3^{(r)}(t) \circ \boldsymbol{\gamma}_4^{(r)}(t), \quad (8)$$

where the vectors $\boldsymbol{\gamma}_h^{(r)}(t) = \boldsymbol{\gamma}_{h,s_t}^{(r)}$, $h = 1, \dots, 4$, $r = 1, \dots, R$, are called the marginals of the PARAFAC decomposition and have length I , J , K and Q , respectively. See Appendix A and the supplement for further details. This specification permits us to: (i) achieve parsimony of the model, since for each value of the state s_t the dimension of the parametric

space is reduced from $IJKQ$ to $R(I + J + K + Q)$; (ii) introduce sparsity in the coefficient tensor, through a suitable choice of the prior distribution for the PARAFAC marginals.

3 Bayesian Inference

As regards the prior distributions for the parameters of interest, we choose the following specifications. We assume a global-local shrinkage prior for on $\gamma_{h,l}^{(r)}$

$$p(\gamma_{h,l}^{(r)} | \bar{\zeta}_{h,l}^r, \tau, \phi_r, w_{h,r,l}) \sim \mathcal{N}_{n_h}(\bar{\zeta}_{h,l}^r, \tau \phi_r w_{h,r,l} \mathbf{I}_{n_h}) \quad (9)$$

for $r = 1, \dots, R$, each $h = 1, \dots, 4$ and each $l = 1, \dots, L$, where $n_1 = I$, $n_2 = J$, $n_3 = K$, $n_4 = Q$. The parameter τ represents the global component of the variance, common to all marginals, ϕ_r is the level component and $w_{h,r}$ is the local component. The choice of a global-local shrinkage prior, as opposed to a spike-and-slab distribution, is motivated by the reduced computational complexity and the capacity to handle high-dimensional settings. In what follows we denote with $p(\mathcal{G} | \mathcal{W}, \phi, \tau)$ the joint prior of the $\gamma_{h,l}^{(r)}$, where $\mathcal{W} = \{w_{h,r,l}\}_{h,r,l}$. We assume the following hyperpriors for the variance components¹:

$$p(\tau) \sim \mathcal{Ga}(\bar{a}^\tau, \bar{b}^\tau) \quad \bar{a}^\tau = \bar{\alpha} R \quad (10)$$

$$p(\phi) \sim \mathcal{Dir}(\bar{\alpha}) \quad \bar{\alpha} = \bar{\alpha} \boldsymbol{\iota}_R \quad (11)$$

$$p(w_{h,r,l} | \lambda_l) \sim \mathcal{Exp}(\lambda_l^2 / 2) \quad \forall h, r, l \quad (12)$$

$$p(\lambda_l) \sim \mathcal{Ga}(\bar{a}_l^\lambda, \bar{b}_l^\lambda) \quad \forall l, \quad (13)$$

where $\boldsymbol{\iota}_n$ is the n -dimensional vector of ones. The further level of hierarchy for the local components $w_{h,r,l}$ is added with the aim of favouring information sharing across local components of the variance (indices h and r) within a given regime l . The specification of an exponential distribution for the local component of the variance of the $\gamma_{h,l}^{(r)}$ yields a

¹We use the shape-rate formulation for the gamma distribution, such that $\mathbb{E}(x) = \alpha/\beta$, $\text{Var}(x) = \alpha/\beta^2$.

Laplace (or Double Exponential) distribution for each component of the vectors once the $w_{h,r,l}$ is integrated out, that is $\gamma_{h,l,i}^{(r)}|\lambda_l, \tau, \phi_r \sim \text{Laplace}(0, \lambda_l/\sqrt{\tau\phi_r})$ for all $i = 1, \dots, n_h$. The marginal distribution of each entry, integrating all remaining random components, is a generalized Pareto distribution, which favours sparsity.

In logit models it is not possible to identify the coefficients of the latent regression equation as well as the variance of the noise. As a consequence, we make the usual identifying restriction by imposing unitary variance for each $\varepsilon_{ijk,t}$.

The mixing probability of the observation model is assumed beta distributed:

$$p(\rho_l) \sim \mathcal{Be}(\bar{a}_l^\rho, \bar{b}_l^\rho) \quad \forall l. \quad (14)$$

A well known identification issue for mixture models is the label switching problem (e.g., see [21]). When the specific application provides meaningful restrictions on the value of some parameters (e.g., from theory, or interpretation), they can be used for identifying the regimes. Following this approach, we assume $\rho_1 > \rho_2 > \dots > \rho_L$, meaning that regime 1 represents the sparsest and regime L the densest. Finally, we assume each row of the transition matrix $\boldsymbol{\xi}_l$ follows a Dirichlet distribution

$$p(\boldsymbol{\xi}_l) \sim \mathcal{Dir}(\bar{\mathbf{c}}_l) \quad \forall l. \quad (15)$$

The overall structure of the hierarchical prior distribution is represented graphically by means of the directed acyclic graph in Fig. 1.

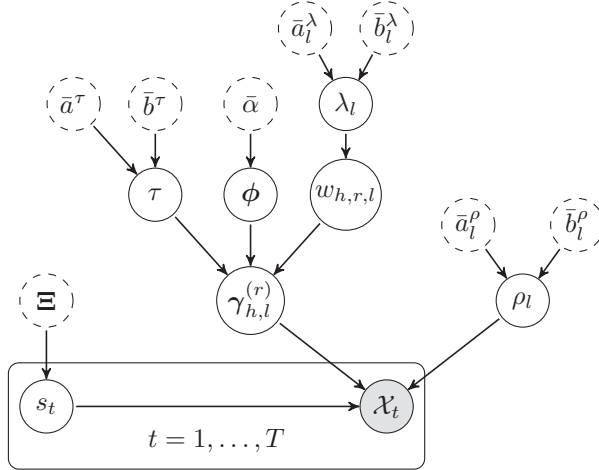


Figure 1: Directed acyclic graph of the model in eq. (6) and prior structure in eq. (9)-(15). Gray circles denote observable variables, white solid circles indicate parameters, white dashed circles indicate fixed hyperparameters. Directed edges represent the conditional independence relationships.

4 Posterior Approximation

Since the joint posterior is not tractable, we apply Markov chain Monte Carlo (MCMC) combined with a data augmentation strategy ([51]). We introduce allocation variables for the mixture in eq. (2) and the Pólya-Gamma augmentation of [43], which allows for conjugate full conditional distributions and a better mixing of the MCMC chain. See also [53] and [30] for an application of the Pólya-Gamma scheme to network-response regression and hidden Markov models, respectively. Define $\boldsymbol{\mathcal{X}} = \{\mathcal{X}_t\}_{t=1}^T$, $\mathbf{s} = \{s_t\}_{t=0}^T$ and let $\boldsymbol{\theta}$ denote the set of parameters. For each $l = 1, \dots, L$, we define $\mathcal{T}_l = \{t : \zeta_{t,l} = 1\}$ and $T_l = \#\mathcal{T}_l$. The data augmented likelihood of the model in eq. (6) is

$$L(\boldsymbol{\mathcal{X}}, \mathbf{s} | \boldsymbol{\theta}) = L(\boldsymbol{\mathcal{X}} | \mathbf{s}, \boldsymbol{\theta}) L(\mathbf{s} | \boldsymbol{\theta}), \quad (16)$$

where

$$L(\mathcal{X}|\mathbf{s}, \boldsymbol{\theta}) = \prod_{l=1}^L \prod_{t \in \mathcal{T}_l} \prod_{i=1}^I \prod_{j=1}^J \prod_{k=1}^K \left(\frac{(1 - \rho_l) \exp(\mathbf{z}'_t \mathbf{g}_{ijk,l})}{1 + \exp(\mathbf{z}'_t \mathbf{g}_{ijk,l})} \right)^{x_{ijk,t}} \left(\rho_l + \frac{1 - \rho_l}{1 + \exp(\mathbf{z}'_t \mathbf{g}_{ijk,l})} \right)^{1 - x_{ijk,t}} \quad (17)$$

and

$$L(\mathbf{s}|\boldsymbol{\theta}) = \prod_{g=1}^L \prod_{l=1}^L \xi_{g,l}^{N_{gl}(\mathbf{s})}, \quad (18)$$

with $N_{gl}(\mathbf{s}) = \#\{\zeta_{t-1,g} = 1, \zeta_{t,l} = 1, t = 1, \dots, T\}$, $g, l = 1, \dots, L$, with $\#$ the cardinality of a set. To make the likelihood more tractable, we further augment the data in two steps. First, we introduce the latent allocation variable for the mixture in eq. (2), $d_{ijk,t} \in \{0, 1\}$, and obtain the conditional distribution

$$p(x_{ijk,t} | d_{ijk,t}, s_t = l, \mathcal{G}_l) = (\delta_{\{0\}}(x_{ijk,t}))^{d_{ijk,t}} \frac{(\exp(\mathbf{z}'_t \mathbf{g}_{ijk,l}))^{x_{ijk,t}(1-d_{ijk,t})}}{(1 + \exp(\mathbf{z}'_t \mathbf{g}_{ijk,l}))^{(1-d_{ijk,t})}}, \quad (19)$$

and the marginal distribution

$$p(d_{ijk,t} | s_t = l, \rho_l) = \rho_l^{d_{ijk,t}} (1 - \rho_l)^{1 - d_{ijk,t}}. \quad (20)$$

Second, we decompose the ratio in eq. (19) and obtain

$$p(x_{ijk,t} | d_{ijk,t}, \omega_{ijk,t}, s_t = l, \mathcal{G}_l) = \frac{(2\delta_{\{0\}}(x_{ijk,t}))^{d_{ijk,t}}}{2} \exp\left(-\frac{\omega_{ijk,t}}{2}(\mathbf{z}'_t \mathbf{g}_{ijk,l})^2 + \kappa_{ijk,t}(\mathbf{z}'_t \mathbf{g}_{ijk,l})\right), \quad (21)$$

where $\kappa_{ijk,t} = (1 - d_{ijk,t})(x_{ijk,t} - 1/2)$ and $\omega_{ijk,t} \sim PG(1, 0)$, with $PG(b, c)$ the Pólya-Gamma distribution with parameters $b > 0$ and $c \in \mathbb{R}$ [?,]Theorem 1]Polsonetal13PolyaGamma.

Defining $\mathcal{D} = \{d_{ijk,t}\}_{ijk,t}$ and $\boldsymbol{\Omega} = \{\omega_{ijk,t}\}_{ijk,t}$ and combining the previous steps one gets the complete data likelihood

$$L(\mathcal{X}, \mathcal{D}, \boldsymbol{\Omega}, \mathbf{s}|\boldsymbol{\theta}) = \left(\prod_{t=1}^T \prod_{i=1}^I \prod_{j=1}^J \prod_{k=1}^K p(\omega_{ijk,t}) \right) \cdot \left(\prod_{g=1}^L \prod_{l=1}^L \xi_{g,l}^{N_{gl}(\mathbf{s})} \right)$$

$$\prod_{l=1}^L \prod_{t \in \mathcal{T}_l} \prod_{i=1}^I \prod_{j=1}^J \prod_{k=1}^K \left(\frac{2\rho_l \delta_{\{0\}}(x_{ijk,t})}{1 - \rho_l} \right)^{d_{ijk,t}} \frac{1 - \rho_l}{2} \exp \left(- \frac{\omega_{ijk,t}}{2} (\mathbf{z}'_t \mathbf{g}_{ijk,l})^2 + \kappa_{ijk,t} (\mathbf{z}'_t \mathbf{g}_{ijk,l}) \right). \quad (22)$$

In the following, we define $\mathcal{G} = \{\mathcal{G}_l\}_{l=1}^L$ and $\boldsymbol{\rho} = \{\rho_l\}_{l=1}^L$, and let \mathbf{W}_l and $\mathbf{W}^{(r)}$ be the $(4 \times R)$ and $(4 \times L)$ matrices representing the l - and r -th slices of \mathcal{W} , along the third and second mode, respectively. The complete data likelihood and the prior distributions yield a posterior sampling scheme consisting of four blocks (see the supplement for the derivation of the posterior full conditional distributions).

In block (I) the sampler draws the latent variables from the full conditional distribution:

$$p(\mathbf{s}, \mathcal{D}, \boldsymbol{\Omega} | \mathcal{X}, \mathcal{G}, \boldsymbol{\Xi}, \boldsymbol{\rho}) = p(\mathbf{s} | \mathcal{X}, \mathcal{G}, \boldsymbol{\Xi}, \boldsymbol{\rho}) p(\mathcal{D} | \mathcal{X}, \mathcal{G}, \boldsymbol{\rho}, \mathbf{s}) p(\boldsymbol{\Omega} | \mathcal{X}, \mathcal{G}, \boldsymbol{\rho}, \mathbf{s}). \quad (23)$$

Samples of \mathbf{s} are drawn via the Forward Filter Backward Sampler (see ch.13 of [22]). The latent variables $\omega_{ijk,t}$ are sampled independently from

$$p(\omega_{ijk,t} | x_{ijk,t}, s_t, \mathcal{G}_{s_t}) \propto PG(1, \mathbf{z}'_t \mathbf{g}_{ijkq, s_t}). \quad (24)$$

The latent variables $\omega_{ijk,t}$ are sampled in block for each t . The latent variables $d_{ijk,t}$ are sampled independently from

$$\begin{aligned} p(d_{ijk,t} = 1 | x_{ijk,t}, s_t, \mathcal{G}_{s_t}, \rho_{s_t}) &\propto \rho_{s_t} \delta_{\{0\}}(x_{ijk,t}) \\ p(d_{ijk,t} = 0 | x_{ijk,t}, s_t, \mathcal{G}_{s_t}, \rho_{s_t}) &\propto (1 - \rho_{s_t}) \frac{\exp((\mathbf{z}'_t \mathbf{g}_{ijkq, s_t}) x_{ijk,t})}{1 + \exp(\mathbf{z}'_t \mathbf{g}_{ijkq, s_t})}. \end{aligned} \quad (25)$$

The hyperparameters which control the variance of the PARAFAC marginals are sampled in block (II) from the full conditional distribution

$$p(\tau, \boldsymbol{\phi}, \mathcal{W} | \{\boldsymbol{\gamma}_{h,l}^{(r)}\}_{h,l,r}) = p(\boldsymbol{\phi} | \{\boldsymbol{\gamma}_{h,l}^{(r)}\}_{h,l,r}, \mathcal{W}) p(\tau | \{\boldsymbol{\gamma}_{h,l}^{(r)}\}_{h,l,r}, \mathcal{W}, \boldsymbol{\phi}) p(\mathcal{W} | \{\boldsymbol{\gamma}_{h,l}^{(r)}\}_{h,l,r}, \boldsymbol{\phi}, \tau). \quad (26)$$

We enable better mixing by blocking together the parameters $\boldsymbol{\phi}$. We set $\phi_r = \psi_r / (\psi_1 + \dots + \psi_R)$, where the auxiliary variables ψ_r are sampled independently for each r from

$$p(\psi_r | \{\boldsymbol{\gamma}_{h,1}^{(r)}\}_{h,l}, \mathbf{W}^{(r)}) \propto \text{GiG} \left(2\bar{b}^\tau, \sum_{h=1}^4 \sum_{l=1}^L \frac{\boldsymbol{\gamma}_{h,l}^{(r)'} \boldsymbol{\gamma}_{h,l}^{(r)}}{w_{h,r,l}}, \bar{\alpha} - n \right), \quad (27)$$

where $\text{GiG}(a, b, p)$ is Generalized Inverse Gaussian distribution with parameters $p \in \mathbb{R}$, $a > 0$ and $b > 0$, and $n = \sum_{h=1}^4 n_h$. The global variance parameter τ is drawn from

$$p(\tau | \{\boldsymbol{\gamma}_{h,l}^{(r)}\}_{h,l,r}, \mathcal{W}, \boldsymbol{\phi}) \propto \text{GiG}\left(2\bar{b}^\tau, \sum_{r=1}^R \sum_{h=1}^4 \sum_{l=1}^L \frac{\boldsymbol{\gamma}_{h,l}^{(r)\prime} \boldsymbol{\gamma}_{h,l}^{(r)}}{\phi_r w_{h,r,l}}, (\bar{a} - n)R\right). \quad (28)$$

The local variance parameters $w_{h,r,l}$ are independently drawn from

$$p(w_{h,r,l} | \boldsymbol{\gamma}_{h,l}^{(r)}, \phi_r, \tau, \lambda_l) \propto \text{GiG}\left(\lambda_l^2, \frac{\boldsymbol{\gamma}_{h,l}^{(r)\prime} \boldsymbol{\gamma}_{h,l}^{(r)}}{\tau \phi_r}, 1 - \frac{n_h}{2}\right). \quad (29)$$

Finally, the hyperparameters λ_l are independently drawn from

$$p(\lambda_l | \mathbf{W}_l) \propto \lambda_l^{\bar{a}_l + 8R - 1} \exp\left(-\lambda_l \bar{b}_l - \frac{\lambda_l^2}{2} \sum_{r=1}^R \sum_{h=1}^4 w_{h,r,l}\right). \quad (30)$$

Block (III) concerns the marginals of the PARAFAC decomposition for the tensors \mathcal{G}_l . The vectors $\boldsymbol{\gamma}_{h,l}^{(r)}$ are sampled independently from

$$p(\boldsymbol{\gamma}_{h,l}^{(r)} | \mathcal{X}, \mathcal{W}, \boldsymbol{\phi}, \tau, \mathbf{s}, \mathcal{D}, \boldsymbol{\Omega}) \propto \mathcal{N}_{n_h}\left(\tilde{\boldsymbol{\zeta}}_{h,l}^r, \tilde{\boldsymbol{\Lambda}}_{h,l}^r\right). \quad (31)$$

Finally, in block (IV) are drawn the mixing probability ρ_l and the row $\boldsymbol{\xi}_l$ of the transition matrix $\boldsymbol{\Xi}$ from

$$p(\rho_l | \mathcal{D}, \mathbf{s}) \propto \mathcal{B}e(\tilde{a}_l^\rho, \tilde{b}_l^\rho), \quad (32)$$

$$p(\boldsymbol{\xi}_l | \mathbf{s}) \propto \mathcal{D}ir(\tilde{\mathbf{c}}). \quad (33)$$

Blocks (I) and (II) are Rao-Blackwellized Gibbs steps: in block (I) we have marginalised over both $(\mathcal{D}, \boldsymbol{\Omega})$ in the full joint conditional distribution of the state \mathbf{s} and \mathcal{D} (together with $\boldsymbol{\rho}$) in the full conditional of $\boldsymbol{\Omega}$, while in (II) we have integrated out τ from the full conditional of $\boldsymbol{\phi}$. The derivation of the full conditional distributions is given in Appendix B. The supplement provides details on the Gibbs sampler and the results of a simulation study in which we show the efficiency of the proposed MCMC and its effectiveness in recovering the true value of the latent Markov chain and parameters.

5 Empirical Application

We apply the proposed methodology to temporal financial networks for European institutions obtained as in [7]. The application is appealing since there are few empirical studies on this dataset and, to the best of our knowledge, none of them considers a dynamic network model. The dataset consists of 110 binary, directed networks estimated at the monthly frequency, from December 2003 to January 2013, by Granger² causality³, where the nodes are 61 European financial institutions (25 banks, 11 insurance companies and 25 investment companies, in this order). $x_{ij,t} = 1$ represents a Granger-causal link from institution i to institution j at time t . The most striking features of the data are time-varying sparsity (see Fig. 2) and temporal clustering of sparse and dense network topologies (see the supplement for a representation of the temporal network dataset).



Figure 2: Graphical representation of networks at time $t = 25$ (Dec 2005), $t = 43$ (Jul 2007) and $t = 69$ (Aug 2009), respectively. Node size is proportional to its total degree. Edge (i, j) is clockwise oriented when i Granger causes j .

The set of covariates \mathbf{z}_t used to explain each edge's probability includes a constant term and some risk factors usually employed in empirical finance: the monthly change of the

²See e.g. [49], [9].

³We define a binary adjacency matrix for each month by setting an entry to 1 only if the corresponding Granger-causality link existed for the whole month (i.e. for each trading day of the corresponding month), and setting the entry to 0 otherwise.

VSTOXX index (DVX), the monthly log-returns on the STOXX50 index (STX), the credit spread (CRS), the term spread (TRS) and the momentum factor (MOM). In addition, we include a connectedness risk measure to account for financial linkages persistence: the network total degree (DTD). All covariates have been standardised and included with one lag, except DVX which is contemporaneous, following the standard practice (e.g., see [39]).

We estimated the model in eq. (6) with tensor rank $R = 5$, $L = 2$ regimes and use the Gibbs sampler of section 4 to obtain 5,000 draws from the posterior, after thinning and burn-in. See the supplement for details about the initialization.

For comparison purposes, we estimate a restricted model which does not allow for heterogeneous effects of the covariates within each regime. The model is obtained by pooling parameters cross-edges for each covariate, $\mathbf{g}_{ijk,l} = \mathbf{g}_l \in \mathbb{R}^Q$, for each i, j, k, l , and by assuming the prior distributions (see Appendix C and supplement for posteriors)

$$\mathbf{g}_l | \tau, w_l \sim \mathcal{N}_Q(\bar{\zeta}_l, \tau w_l \mathbf{I}_Q), \quad w_l | \lambda_l \sim \text{Exp}(\lambda_l^2/2), \quad \lambda_l \sim \mathcal{G}a(\bar{a}_l^\lambda, \bar{b}_l^\lambda), \quad \tau \sim \mathcal{G}a(\bar{a}^\tau, \bar{b}^\tau).$$

In both models the identification constraint $\rho_1 > \rho_2$ allows us to label state 1 and 2 as the sparse and dense regime, respectively.

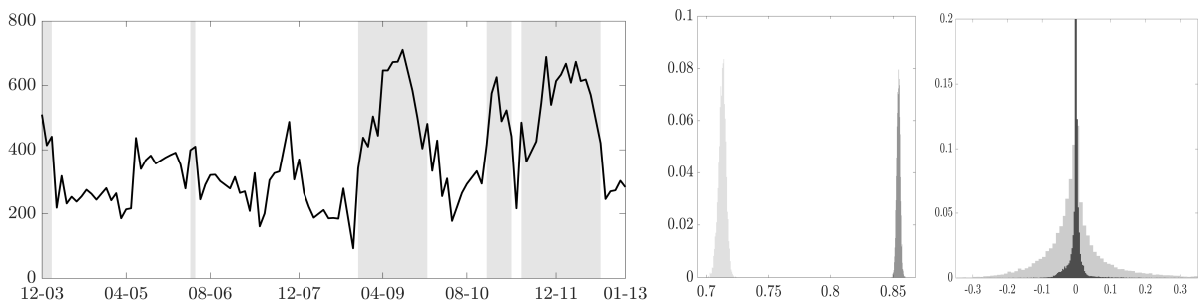


Figure 3: In all plots light (dark) grey identifies the dense (sparse) regime. *Left*: total degree of the temporal network (*line*) and estimated regimes (*vertical bars*) over time (format *mm-yy*). *Middle*: posterior distribution of the sparsity parameters ρ_1 and ρ_2 . *Right*: distribution of the entries of the estimated coefficient tensor.

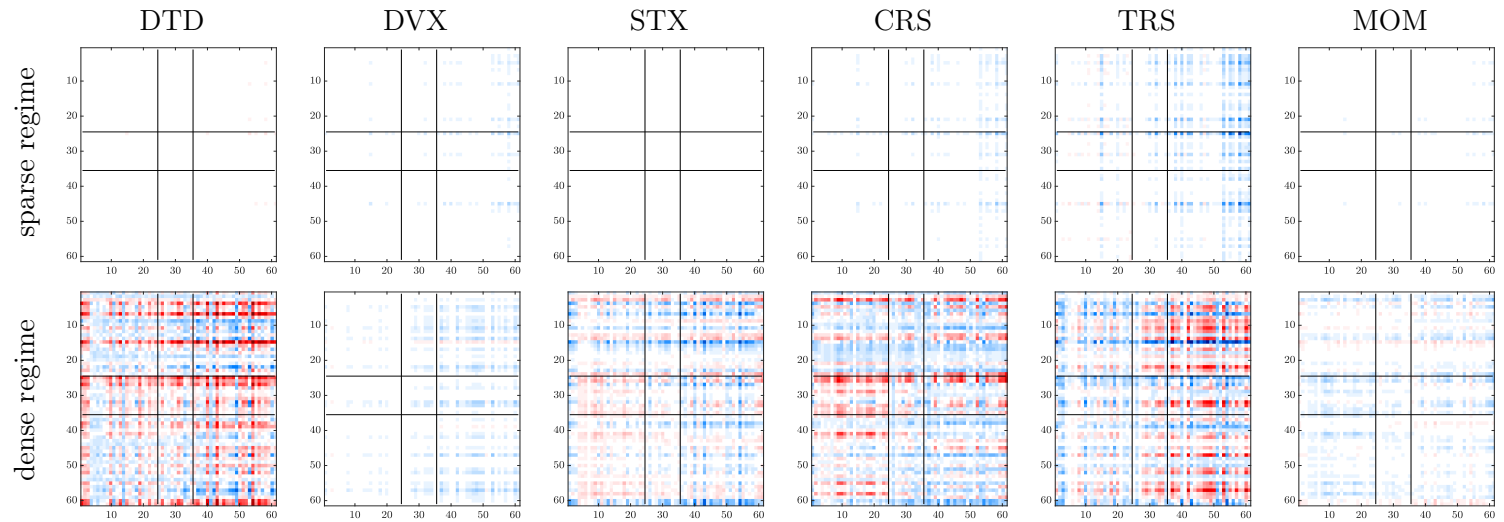


Figure 4: Posterior mean of the coefficient tensor, in matricised form, in the sparse (*top*) and dense (*bottom*) state of the hidden Markov chain. In each plot, entry (i, j) represents the effect of the covariate reported in column on the probability of observing the edge between institution i and institution j . Black lines separate groups of institutions: banks (i and j in $\{1, \dots, 25\}$), insurance ($\{26, \dots, 36\}$) and investment companies ($\{37, \dots, 61\}$). Same color scale, with red, blue and white colors indicating positive, negative and zero valued coefficients, respectively.

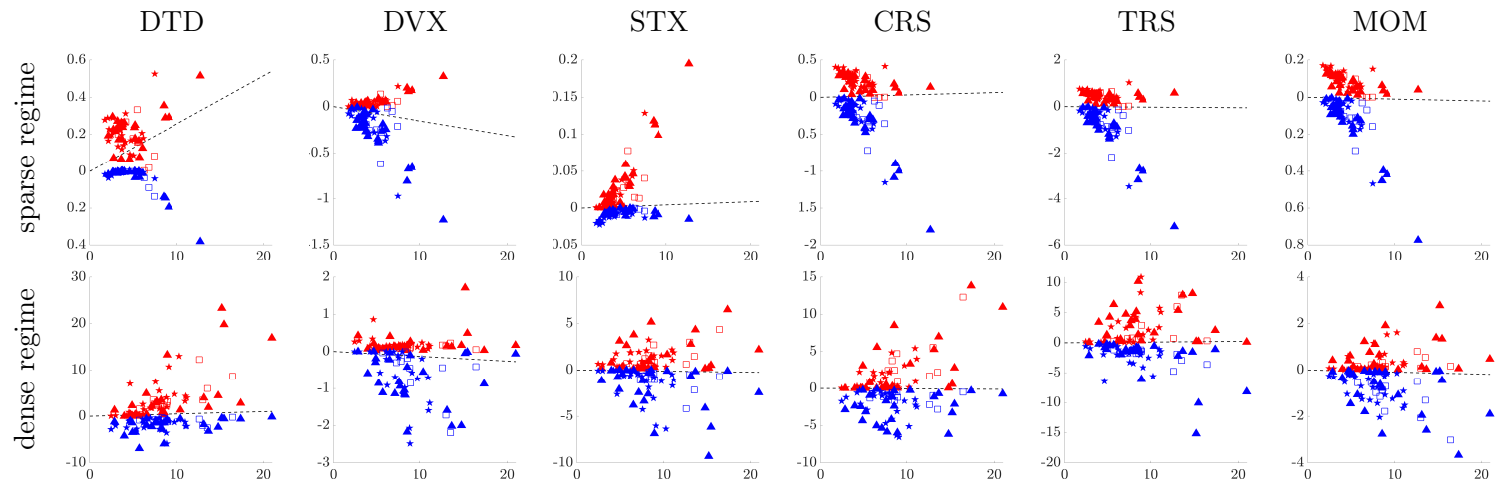


Figure 5: Covariate coefficients (columns) for the incoming edge probabilities in the two regimes (rows). In each scatterplot: total node degree averaged over time within each regime (horizontal axis) versus the sum of the negative (blue) and positive (red) node coefficients of a given variable (vertical axis). Nodes: banks (\blacktriangle , \blacktriangle), insurance companies (\square , \square) and investment companies (\star , \star). Dashed line: the sum of the coefficients for the pooled model.

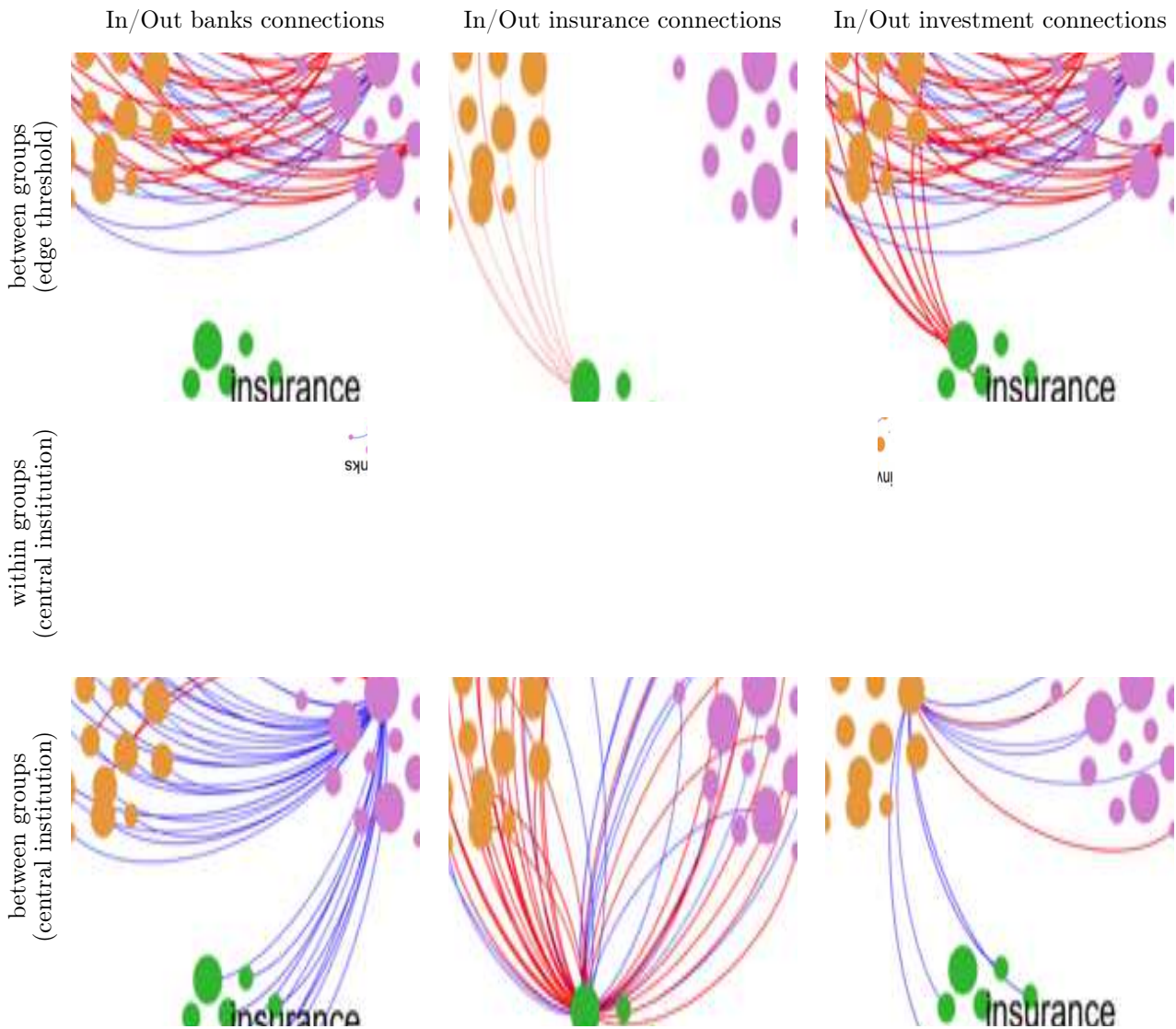


Figure 6: TRS coefficients in the dense regime. In the columns the effect of TRS on the edges from and to a specific group of nodes: bank (purple), insurance (green), investment companies (orange). In the rows the effects of TRS on between and within groups connectivity, filtering relevant effects (first row) and central institutions (second and third row). Node size: proportional to the total degree averaged over time within each regime. Edge color: blue for negative, red for positive. We show only edges with significant TRS coefficient.

The estimated regimes are given in the left plot of Fig. 3 together with the network total degree. The identification constraint permits to recognise low and high connectedness periods and is strongly supported by the data, since the posterior distributions are well separated (middle plot). The distribution of the estimated coefficients in the two regimes (right plot) highlights the higher heterogeneity across edges in the dense regime. The unrestricted tensor model captures the edge-specific impact of each risk factor (different colors in each plot of Fig. 4) as opposed to the pooled model (see Fig. ?? in the supplement), and allows us to provide new insights on the dynamic relationship among financial institutions and risk factors. In the dense regime, we find that the credit spread positively affects the probability to be connected to banks from all institutions, and a negative impact on the edge probabilities among investment companies. The term spread has a strong positive effect on connecting to insurance and investment companies, and from banks to insurances. Similarly, the stock index return positively affects the edge probability from insurance and investment companies to banks. We find also that the autoregressive term has an average positive effect, which might account for either connectedness risk persistence or spurious autocorrelation due to the network estimation step.

In the sparse regime (first line of Fig. 4) there is no evidence of impact for almost all covariates. This is most striking for CRS, TRS and DTD, which are the most relevant predictors in the dense state. This finding supports the stylised fact that the risk factors have higher explanatory power in periods of higher connectivity of the financial network ([7]).

Fig. 5 allows to detect potential relationships between covariate effects and node degree centrality. In particular, we find evidence of positive relationship (in absolute value) for DTD, CRS, TRS and MOM. In the sparse regime, all institutions feature low average degree and there is evidence of a weaker relationship for CRS, TRS, and negative impact for MOM. In the dense regime, the most central institutions (banks and insurance) are the

most affected both in terms of the number of connections and the risk factor impact (see the top- and bottom-right part of the scatterplots in Fig. 5). Furthermore, according to the estimated regimes, the most central institutions differ between regimes (see node size in Fig. 6), with banks being the more connected in both states.

We focus on the term spread factor, since it is a key variable for monetary policy analysis. The unrestricted tensor model provides interesting results on the effect of term spread on the different types of institutions, especially in the dense regime. We disentangle the relationship among institutions by highlighting the most affected linkages (first row of Fig. 6) and the impact on all the linkages of the most central nodes (second and third row). We find that the term spread mostly increases edge probability from banks and the most central insurance company to investment companies. There is no evidence of relevant impact on linkages between banks and insurances, which are strongly affected by the credit spread (see the supplement for further results). Finally, the effect of the term spread is larger for between group connectivity than for within group connectivity. Most of the edges of the central investment company and bank are negatively affected by the term spread (left and right plots), whereas the connectivity of the central insurance company increases with the term spread (middle plot).

6 Summary and Concluding Remarks

We present a new zero-inflated logit regression for time series of binary tensors, such as the connectivity tensors encoding the dependence structure of multilayer networks. The mixing probability allows to capture the sparsity pattern in the data, and a set of coefficient tensors captures the effect of the covariates on each binary observation. We propose a parsimonious parametrization based on the PARAFAC decomposition of the coefficient tensor and allow the regression parameters to switch between multiple regimes in order to capture the time-

varying sparsity patterns.

We consider the Bayesian paradigm in the inferential process and developed an efficient Gibbs sampler for posterior approximation. We analyze a real dataset of time-varying networks among European financial institutions. There is strong evidence of heterogeneous effects of the covariates across edges and regimes, with the term spread and credit spread factors playing an important role in explaining the connectivity of central institutions. Our new empirical results can give interesting insights to policy makers for financial stability and risk monitoring.

Supplementary Materials

Background material on tensors, the derivation of the posterior, simulation experiments and the description of the data are given in an online supplement⁴.

References

- [1] Daron Acemoglu, Vasco M Carvalho, Asuman Ozdaglar, and Alireza Tahbaz-Salehi. The network origins of aggregate fluctuations. *Econometrica*, 80(5):1977–2016, 2012.
- [2] Daniel Felix Ahelegbey, Monica Billio, and Roberto Casarin. Bayesian graphical models for structural vector autoregressive processes. *Journal of Applied Econometrics*, 31(2):357–386, 2016.
- [3] Daniel Felix Ahelegbey, Monica Billio, and Roberto Casarin. Sparse graphical vector autoregression: a Bayesian approach. *Annals of Economics and Statistics/Annales d'Économie et de Statistique*, (123/124):333–361, 2016.

⁴https://matteoiacopini.github.io/docs/BiCaIa_Supplement.pdf

- [4] Onureena Banerjee, Laurent El Ghaoui, and Alexandre d’Aspremont. Model selection through sparse maximum likelihood estimation for multivariate gaussian or binary data. *Journal of Machine Learning Research*, 9(Mar):485–516, 2008.
- [5] Lindsay R Berry and Mike West. Bayesian forecasting of many count-valued time series. *Journal of Business & Economic Statistics*, (forthcoming):1–34, 2019.
- [6] Daniele Bianchi, Monica Billio, Roberto Casarin, and Massimo Guidolin. Modeling systemic risk with Markov switching graphical SUR models. *Journal of Econometrics*, 2010(1):58–74, 2019.
- [7] Monica Billio, Mila Getmansky, Andrew W Lo, and Lorian Pelizzon. Econometric measures of connectedness and systemic risk in the finance and insurance sectors. *Journal of Financial Economics*, 104(3):535–559, 2012.
- [8] Stefano Boccaletti, Ginestra Bianconi, Regino Criado, Charo I Del Genio, Jesús Gómez-Gardenes, Miguel Romance, Irene Sendina-Nadal, Zhen Wang, and Massimiliano Zanin. The structure and dynamics of multilayer networks. *Physics Reports*, 544(1):1–122, 2014.
- [9] Hafida Boudjellaba, Jean-Marie Dufour, and Roch Roy. Testing causality between two vectors in multivariate autoregressive moving average models. *Journal of the American Statistical Association*, 87(420):1082–1090, 1992.
- [10] Carlos M Carvalho, Jeffrey Chang, Joseph E Lucas, Joseph R Nevins, Quanli Wang, and Mike West. High-dimensional sparse factor modeling: applications in gene expression genomics. *Journal of the American Statistical Association*, 103(484):1438–1456, 2008.
- [11] Carlos M Carvalho, Mike West, et al. Dynamic matrix-variate graphical models. *Bayesian Analysis*, 2(1):69–97, 2007.

- [12] Roberto Casarin, Domenico Sartore, and Marco Tronzano. A Bayesian Markov-switching correlation model for contagion analysis on exchange rate markets. *Journal of Business & Economic Statistics*, 36(1):101–114, 2018.
- [13] Thomas Chaney. The network structure of international trade. *The American Economic Review*, 104(11):3600–3634, 2014.
- [14] Xi Chen, Kaoru Irie, David Banks, Robert Haslinger, Jewell Thomas, and Mike West. Scalable bayesian modeling, monitoring, and analysis of dynamic network flow data. *Journal of the American Statistical Association*, 113(522):519–533, 2018.
- [15] Siddhartha Chib, Federico Nardari, and Neil Shephard. Markov Chain Monte Carlo methods for stochastic volatility models. *Journal of Econometrics*, 108(2):281–316, 2002.
- [16] Nicholas A Christakis and James H Fowler. The collective dynamics of smoking in a large social network. *New England Journal of Medicine*, 358(21):2249–2258, 2008.
- [17] A Cichocki, N Lee, IV Oseledets, AH Phan, Q Zhao, and D Mandic. Tensor networks for dimensionality reduction and large-scale optimization: Part 1 low-rank tensor decompositions. *Foundations and Trends in Machine Learning*, 9(4-5):249–429, 2016.
- [18] Andrzej Cichocki, Danilo Mandic, Lieven De Lathauwer, Guoxu Zhou, Qibin Zhao, Cesar Caiafa, and Huy Anh Phan. Tensor decompositions for signal processing applications: From two-way to multiway component analysis. *IEEE Signal Processing Magazine*, 32(2):145–163, 2015.
- [19] Francis X Diebold and Kamil Yilmaz. On the network topology of variance decompositions: measuring the connectedness of financial firms. *Journal of Econometrics*, 182(1):119–134, 2014.

- [20] Daniele Durante and David B. Dunson. Bayesian logistic Gaussian process models for dynamic networks. *Proceedings of the 17th International Conference on Artificial Intelligence and Statistics (AISTATS)*, 33, 2014.
- [21] Sylvia Frühwirth-Schnatter. Markov Chain Monte Carlo estimation of classical and dynamic switching and mixture models. *Journal of the American Statistical Association*, 96(453):194–209, 2001.
- [22] Sylvia Frühwirth-Schnatter. *Finite mixture and Markov switching models*. Springer, 2006.
- [23] Liudas Giraitis, George Kapetanios, Anne Wetherilt, and Filip Žikeš. Estimating the dynamics and persistence of financial networks, with an application to the Sterling money market. *Journal of Applied Econometrics*, 31(1):58–84, 2016.
- [24] Bryan S Graham. An econometric model of network formation with degree heterogeneity. *Econometrica*, 85(4):1033–1063, 2017.
- [25] Rajarshi Guhaniyogi, Shaan Qamar, and David B Dunson. Bayesian tensor regression. *Journal of Machine Learning Research*, 18(79):1–31, 2017.
- [26] Markus Haas, Stefan Mittnik, and Marc S Paoletta. A new approach to Markov-switching GARCH models. *Journal of Financial Econometrics*, 2(4):493–530, 2004.
- [27] Wolfgang Hackbusch. *Tensor spaces and numerical tensor calculus*. Springer Science & Business Media, 2012.
- [28] James D Hamilton. A new approach to the economic analysis of nonstationary time series and the business cycle. *Econometrica*, 57(2):357–384, 1989.
- [29] Petter Holme and Jari Saramäki. Temporal networks. *Physics Reports*, 519(3):97–125, 2012.

- [30] Tracy Holsclaw, Arthur M Greene, Andrew W Robertson, and Padhraic Smyth. Bayesian non-homogeneous Markov models via Pólya-Gamma data augmentation with applications to rainfall modeling. *The Annals of Applied Statistics*, 11(1):393–426, 2017.
- [31] Sylvia Kaufmann. K-state switching models with time-varying transition distributions—Does loan growth signal stronger effects of variables on inflation? *Journal of Econometrics*, 187(1):82–94, 2015.
- [32] Chang-Jin Kim and Charles R Nelson. Business cycle turning points, a new coincident index, and tests of duration dependence based on a dynamic factor model with regime switching. *Review of Economics and Statistics*, 80(2):188–201, 1998.
- [33] Mikko Kivelä, Alex Arenas, Marc Barthelemy, James P Gleeson, Yamir Moreno, and Mason A Porter. Multilayer networks. *Journal of Complex Networks*, 2(3):203–271, 2014.
- [34] Kwangmoo Koh, Seung-Jean Kim, and Stephen Boyd. An interior-point method for large-scale l_1 -regularized logistic regression. *Journal of Machine Learning Research*, 8:1519–1555, 2007.
- [35] Mladen Kolar, Le Song, Amr Ahmed, Eric P Xing, et al. Estimating time-varying networks. *The Annals of Applied Statistics*, 4(1):94–123, 2010.
- [36] Tamara G. Kolda and Brett W. Bader. Tensor decompositions and applications. *SIAM Review*, 51(3):455–500, 2009.
- [37] Pieter M Kroonenberg. *Applied multiway data analysis*. John Wiley & Sons, 2008.

- [38] Willem Kruijer, Judith Rousseau, and Aad Van Der Vaart. Adaptive Bayesian density estimation with location-scale mixtures. *Electronic Journal of Statistics*, 4:1225–1257, 2010.
- [39] Adam A Majewski, Giacomo Bormetti, and Fulvio Corsi. Smile from the past: a general option pricing framework with multiple volatility and leverage components. *Journal of Econometrics*, 187(2):521–531, 2015.
- [40] Angelo Mele. A structural model of dense network formation. *Econometrica*, 85(3):825–850, 2017.
- [41] Radford M Neal. MCMC using Hamiltonian dynamics. In Steve Brooks, Andrew Gelman, Jones L Galin, and Xiao-Li Meng, editors, *Handbook of Markov Chain Monte Carlo*, chapter 5. Chapman & Hall /CRC, 2011.
- [42] Mark Newman. *Networks: an introduction*. Oxford university press, 2010.
- [43] Nicholas G Polson, James G Scott, and Jesse Windle. Bayesian inference for logistic models using Pólya–Gamma latent variables. *Journal of the American Statistical Association*, 108(504):1339–1349, 2013.
- [44] Pradeep Ravikumar, Martin J Wainwright, and John D Lafferty. High-dimensional Ising model selection using l1-regularized logistic regression. *The Annals of Statistics*, 38(3):1287–1319, 2010.
- [45] Jonathan S Schildcrout and Patrick J Heagerty. Regression analysis of longitudinal binary data with time-dependent environmental covariates: bias and efficiency. *Biostatistics*, 6(4):633–652, 2005.

- [46] Michael Sherman, Tatiyana V Apanasovich, and Raymond J Carroll. On estimation in binary autologistic spatial models. *Journal of Statistical Computation and Simulation*, 76(2):167–179, 2006.
- [47] Christopher A Sims, Daniel F Waggoner, and Tao Zha. Methods for inference in large multiple-equation Markov-switching models. *Journal of Econometrics*, 146(2):255–274, 2008.
- [48] Tom AB Snijders, Johan Koskinen, and Michael Schweinberger. Maximum likelihood estimation for social network dynamics. *The Annals of Applied Statistics*, 4(2):567–588, 2010.
- [49] Norman R Swanson and Clive WJ Granger. Impulse response functions based on a causal approach to residual orthogonalization in vector autoregressions. *Journal of the American Statistical Association*, 92(437):357–367, 1997.
- [50] Matt Taddy. Multinomial inverse regression for text analysis. *Journal of the American Statistical Association*, 108(503):755–770, 2013.
- [51] Martin A Tanner and Wing Hung Wong. The calculation of posterior distributions by data augmentation. *Journal of the American Statistical Association*, 82(398):528–540, 1987.
- [52] Maria Vivien Visaya, David Sherwell, Benn Sartorius, and Fabien Cromieres. Analysis of binary multivariate longitudinal data via 2-dimensional orbits: an application to the Agincourt health and socio-demographic surveillance system in South Africa. *PloS one*, 10(4):e0123812, 2015.
- [53] Lu Wang, Daniele Durante, Rex E Jung, and David B Dunson. Bayesian network-response regression. *Bioinformatics*, 33(12):1859–1866, 2017.

- [54] JD Wilbur, JK Ghosh, CH Nakatsu, SM Brouder, and RW Doerge. Variable selection in high-dimensional multivariate binary data with application to the analysis of microbial community DNA fingerprints. *Biometrics*, 58(2):378–386, 2002.
- [55] Jesse Windle, Carlos M Carvalho, et al. A tractable state-space model for symmetric positive-definite matrices. *Bayesian Analysis*, 9(4):759–792, 2014.
- [56] Yu Ryan Yue, Martin A Lindquist, and Ji Meng Loh. Meta-analysis of functional neuroimaging data using Bayesian nonparametric binary regression. *The Annals of Applied Statistics*, 6(2):697–718, 2012.
- [57] Arnold Zellner. An efficient method of estimating seemingly unrelated regressions and tests for aggregation bias. *Journal of the American Statistical Association*, 57(298):348–368, 1962.

A Background Material on Tensors

This appendix provides the main definitions used in the paper. See the supplement for further results. We introduce some notation for multilinear arrays (i.e. tensors), some basic operations defined on them and lower dimensional objects (such as matrices and vectors) and two tensor decompositions (see [36], [17] for a noteworthy introduction to these topics). The *order* of a tensor is the number of dimensions, or modes (i.e., a matrix is a 2-order tensor). The *mode- k fiber* of D -order tensor \mathcal{X} is the vector obtained along the dimension k by fixing all the other dimensions, that is

$$\mathcal{X}_{(i_1, \dots, i_{k-1}, :, i_{k+2}, \dots, i_D)}. \quad (\text{A.1})$$

Similarly, *slices* are matrices obtained by fixing all but two or more dimensions (or modes) of the tensor. By convention, we denote a whole dimension of a tensor by the symbol

“:”. The mode- k *matricization* operator, $\mathbf{X}_{(n)}$, transforms a D -array \mathcal{X} into a matrix by rearranging all the mode- n fibers to be the columns of a matrix, which will have size $\mathbf{X}_{(n)} \in \mathbb{R}^{d_n \times \bar{d}_{(-n)}}$ with $\bar{d}_{(-n)} = \prod_{i \neq n} d_i$. The *vectorization* of a tensor consists in stacking all the elements in a unique vector of dimension $\bar{d} = \prod_i d_i$, following the inverse lexicographic order. The *outer product* \circ of two tensors $\mathcal{Y} \in \mathbb{R}^{d_1^Y \times \dots \times d_M^Y}$ and $\mathcal{X} \in \mathbb{R}^{d_1^X \times \dots \times d_N^X}$ is the tensor $\mathcal{Z} \in \mathbb{R}^{d_1^Y \times \dots \times d_M^Y \times d_1^X \times \dots \times d_N^X}$ whose entries are obtained as

$$\mathcal{Z}_{i_1, \dots, i_M, j_1, \dots, j_N} = (\mathcal{Y} \circ \mathcal{X})_{i_1, \dots, i_M, j_1, \dots, j_N} = \mathcal{Y}_{i_1, \dots, i_M} \mathcal{X}_{j_1, \dots, j_N}. \quad (\text{A.2})$$

The *PARAFAC(R) decomposition* is a low rank decomposition that represents a D -order tensor $\mathcal{X} \in \mathbb{R}^{d_1 \times \dots \times d_D}$ as the sum of R rank one tensors, that is, of outer products of vectors (also called marginals):

$$\mathcal{X} = \sum_{r=1}^R \mathcal{X}_r = \sum_{r=1}^R \mathbf{x}_1^{(r)} \circ \dots \circ \mathbf{x}_D^{(r)}, \quad \mathbf{x}_j^{(r)} \in \mathbb{R}^{d_j}. \quad (\text{A.3})$$

B Proofs of the Results in the Paper

This appendix provides the derivation of the results. See the supplement for further details.

B.1 Full conditional distribution of ϕ_r

Let $n = n_1 + n_2 + n_3 + n_4 = I + J + K + Q$, then the posterior full conditional is

$$\begin{aligned} p(\phi | \mathcal{G}, \mathcal{W}) &\propto p(\phi) \int_0^\infty p(\mathcal{G} | \mathcal{W}, \phi, \tau) p(\tau) d\tau \\ &\propto \int_0^\infty \left(\prod_{r=1}^R (\tau \phi_r)^{\bar{\alpha} - n - 1} \right) \exp \left(- \frac{1}{2} \sum_{r=1}^R \left(2\bar{b}^\tau \tau \phi_r + \frac{1}{\tau \phi_r} \sum_{h=1}^4 \sum_{l=1}^L \frac{\gamma_{h,l}^{(r)'} \gamma_{h,l}^{(r)}}{w_{h,r,l}} \right) \right) d\tau. \end{aligned}$$

The integrand is the kernel of the GiG distribution given in eq. (27). Following [25] and [38], it is possible to sample from the posterior of ϕ_r , for each $r = 1, \dots, R$ by first sampling ψ_r , then setting $\phi_r = \psi_r / (\psi_1 + \dots + \psi_R)$.

B.2 Full conditional distribution of τ

The posterior full conditional distribution is

$$\begin{aligned} p(\tau|\mathcal{G}, \mathcal{W}, \phi) &\propto \tau^{\bar{a}\tau-1} \exp(-\bar{b}\tau) \prod_{r=1}^R \prod_{h=1}^4 \prod_{l=1}^L |\tau \phi_r w_{h,r,l} \mathbf{I}_{n_h}|^{-1/2} \exp\left(-\frac{1}{2} \frac{\gamma_{h,l}^{(r)'} \gamma_{h,l}^{(r)}}{\phi_r w_{h,r,l}}\right) \\ &\propto \tau^{\bar{a}\tau-4R-1} \exp\left(-\frac{1}{2} \left(2\bar{b}\tau + \frac{1}{\tau} \sum_{r=1}^R \sum_{h=1}^4 \sum_{l=1}^L \frac{\gamma_{h,l}^{(r)'} \gamma_{h,l}^{(r)}}{\phi_r w_{h,r,l}}\right)\right), \end{aligned}$$

which is the kernel of the GiG in eq. (28).

B.3 Full conditional distribution of $w_{h,r,l}$

The posterior full conditional distribution is

$$\begin{aligned} p(w_{h,r,l}|\gamma_{h,l}^{(r)}, \phi_r, \tau, \lambda_l) &\propto p(w_{h,r,l}|\lambda_l) p(\gamma_{h,l}^{(r)}|w_{h,r,l}, \phi_r, \tau) \\ &\propto \exp\left(-\frac{\lambda_l^2}{2} w_{h,r,l}\right) w_{h,r,l}^{-n_h/2} \exp\left(-\frac{1}{2} \frac{\gamma_{h,l}^{(r)'} \gamma_{h,l}^{(r)}}{\tau \phi_r w_{h,r,l}}\right), \end{aligned}$$

which is the kernel of the GiG in eq. (29).

B.4 Full conditional distribution of λ_l

The posterior full conditional distribution of λ_l is

$$\begin{aligned} p(\lambda_l|\mathbf{W}_l) &\propto \lambda_l^{a_l^\lambda-1} \exp(-b_l^\lambda \lambda_l) \prod_{r=1}^R \prod_{h=1}^4 \frac{\lambda_l^2}{2} \exp\left(-\frac{\lambda_l^2}{2} w_{h,r,l}\right) \\ &\propto \lambda_l^{\bar{a}_l^\lambda+8R-1} \exp\left(-\lambda_l \bar{b}_l^\lambda - \frac{\lambda_l^2}{2} \sum_{r=1}^R \sum_{h=1}^4 w_{h,r,l}\right). \end{aligned}$$

We sample from this distribution using a Hamiltonian Monte Carlo step ([41]).

B.5 Full conditional distribution of $\gamma_{h,l}^{(r)}$

For deriving the full conditional distribution of PARAFAC marginals, $\gamma_{h,l}^{(r)}$, start by defining $u_{ijk,t} = \kappa_{ijk,t}/\omega_{ijk,t}$, $\mathcal{U}_t = (u_{ijk,t})_{ijk}$, $\mathbf{\Omega}_t = (\omega_{ijk,t})_{ijk}$, $\mathbf{u}_t = \text{vec}(\mathcal{U}_t)$ and $\bar{\mathbf{\Omega}}_t = \text{diag}(\text{vec}(\mathbf{\Omega}_t))$. From eq. (21), denoting with $p(\mathcal{G}_l)$ the joint prior distribution on $\{\gamma_{h,l}^{(r)}\}_{h,r}$, one gets

$$p(\mathcal{G}_l | \mathcal{X}_t, \mathcal{D}_t, \mathbf{\Omega}_t, s_t = l, \rho_l) \propto p(\mathcal{G}_l) \prod_{t \in \mathcal{T}_l} \prod_{i=1}^I \prod_{j=1}^J \prod_{k=1}^K p(\omega_{ijk,t}) \cdot \prod_{t \in \mathcal{T}_l} \exp\left(-\frac{1}{2}(\text{vec}(\mathcal{G}_l \times_4 \mathbf{z}_t) - \mathbf{u}_t)' \bar{\mathbf{\Omega}}_t (\text{vec}(\mathcal{G}_l \times_4 \mathbf{z}_t) - \mathbf{u}_t)\right). \quad (\text{B.1})$$

By the definitions of mode- n product and PARAFAC decomposition, denoting by $\langle \cdot, \cdot \rangle$ the standard inner product in the Euclidean space \mathbb{R}^n , we obtain

$$\text{vec}(\mathcal{G}_l \times_4 \mathbf{z}_t) = \sum_{r=1}^R (\gamma_{1,l}^{(r)} \circ \gamma_{2,l}^{(r)} \circ \gamma_{3,l}^{(r)}) \langle \gamma_{4,l}^{(r)}, \mathbf{z}_t \rangle = \sum_{r=1}^R \bar{\mathbf{g}}_{l,t}^{(r)}. \quad (\text{B.2})$$

From eq. (B.2) we have:

$$\bar{\mathbf{g}}_{l,t}^{(r)} = \langle \gamma_{4,l}^{(r)}, \mathbf{z}_t \rangle \text{vec}(\gamma_{1,l}^{(r)} \circ \gamma_{2,l}^{(r)} \circ \gamma_{3,l}^{(r)}) = \text{vec}(\gamma_{1,l}^{(r)} \circ \gamma_{2,l}^{(r)} \circ \gamma_{3,l}^{(r)}) \mathbf{z}_t' \gamma_{4,l}^{(r)} = \mathbf{A}_4 \gamma_{4,l}^{(r)}, \quad (\text{B.3})$$

$$= \langle \gamma_{4,l}^{(r)}, \mathbf{z}_t \rangle (\gamma_{3,l}^{(r)} \otimes \gamma_{2,l}^{(r)} \otimes \mathbf{I}_I) \gamma_{1,l}^{(r)} = \mathbf{A}_1 \gamma_{1,l}^{(r)} \quad (\text{B.4})$$

$$= \langle \gamma_{4,l}^{(r)}, \mathbf{z}_t \rangle (\gamma_{3,l}^{(r)} \otimes \mathbf{I}_J \otimes \gamma_{1,l}^{(r)}) \gamma_{2,l}^{(r)} = \mathbf{A}_2 \gamma_{2,l}^{(r)}, \quad (\text{B.5})$$

$$= \langle \gamma_{4,l}^{(r)}, \mathbf{z}_t \rangle (\mathbf{I}_K \otimes \gamma_{2,l}^{(r)} \otimes \gamma_{1,l}^{(r)}) \gamma_{3,l}^{(r)} = \mathbf{A}_3 \gamma_{3,l}^{(r)}. \quad (\text{B.6})$$

Setting $\bar{\mathbf{g}}_{l,t}^{(-r)} = \sum_{\substack{v=1 \\ v \neq r}}^R \bar{\mathbf{g}}_{l,t}^{(v)}$ we get $\text{vec}(\mathcal{G}_l \times_4 \mathbf{z}_t) = \bar{\mathbf{g}}_{l,t}^{(r)} + \bar{\mathbf{g}}_{l,t}^{(-r)}$. Thus, for each l we get

$$L(\mathcal{X}, \mathcal{D}, \mathbf{\Omega}, \mathbf{s} | \boldsymbol{\theta}) \propto \prod_{t \in \mathcal{T}_l} \exp\left(-\frac{1}{2}(\bar{\mathbf{g}}_{l,t}^{(r)} + \bar{\mathbf{g}}_{l,t}^{(-r)} - \mathbf{u}_t)' \bar{\mathbf{\Omega}}_t (\bar{\mathbf{g}}_{l,t}^{(r)} + \bar{\mathbf{g}}_{l,t}^{(-r)} - \mathbf{u}_t)\right). \quad (\text{B.7})$$

We can now single out a specific component $\mathcal{G}_l^{(r)}$ of the PARAFAC decomposition of the tensor \mathcal{G} , which is incorporated in $\bar{\mathbf{g}}_{l,t}^{(r)}$. For each $l = 1, \dots, L$ we obtain

$$L(\mathcal{X}, \mathcal{D}, \mathbf{\Omega}, \mathbf{s} | \boldsymbol{\theta}) \propto \prod_{t \in \mathcal{T}_l} \exp\left(-\frac{1}{2}\left(\bar{\mathbf{g}}_{l,t}^{(r)'} \bar{\mathbf{\Omega}}_t \bar{\mathbf{g}}_{l,t}^{(r)} - 2(\mathbf{u}_t - \bar{\mathbf{g}}_{l,t}^{(-r)})' \bar{\mathbf{\Omega}}_t \bar{\mathbf{g}}_{l,t}^{(r)}\right)\right). \quad (\text{B.8})$$

B.5.1 Full conditional distribution of $\gamma_{1,l}^{(r)}$

The full conditional distribution of $\gamma_{1,l}^{(r)}$ is obtained from eqs. (B.4) and (B.8), where

$$\bar{\mathbf{g}}_{l,t}^{(r)'} \bar{\mathbf{\Omega}}_t \bar{\mathbf{g}}_{l,t}^{(r)} = \gamma_{1,l}^{(r)'} \left(\bar{\mathbf{\Sigma}}_{1,l,t}^{(r)} \right)^{-1} \gamma_{1,l}^{(r)} \quad (\text{B.9})$$

$$-2(\mathbf{u}_t - \bar{\mathbf{g}}_{l,t}^{(-r)})' \bar{\mathbf{\Omega}}_t \bar{\mathbf{g}}_{l,t}^{(r)} = -2\bar{\boldsymbol{\mu}}_{1,l,t}^{(r)'} \left(\bar{\mathbf{\Sigma}}_{1,l,t}^{(r)} \right)^{-1} \gamma_{1,l}^{(r)}. \quad (\text{B.10})$$

By Bayes' theorem and plugging eq. (B.9) and eq. (B.10) into eq. (B.8) we get

$$p(\gamma_{1,l}^{(r)} | \boldsymbol{\theta}) = \exp \left(-\frac{1}{2} \left(\gamma_{1,l}^{(r)'} \left((\bar{\mathbf{\Lambda}}_{1,l}^r)^{-1} + \sum_{t \in \mathcal{T}_l} \left(\bar{\mathbf{\Sigma}}_{1,l,t}^{(r)} \right)^{-1} \right) \gamma_{1,l}^{(r)} - 2 \left(\bar{\boldsymbol{\zeta}}_{1,l}^{r'} \left(\bar{\mathbf{\Lambda}}_{1,l}^r \right)^{-1} + \sum_{t \in \mathcal{T}_l} \bar{\boldsymbol{\mu}}_{1,l,t}^{(r)'} \left(\bar{\mathbf{\Sigma}}_{1,l,t}^{(r)} \right)^{-1} \right) \gamma_{1,l}^{(r)} \right),$$

that is the kernel of the desired multivariate normal distribution.

B.5.2 Full conditional distribution of $\gamma_{2,l}^{(r)}$

The full conditional distribution of $\gamma_{2,l}^{(r)}$ is obtained from eqs. (B.5) and (B.8), where

$$\bar{\mathbf{g}}_{l,t}^{(r)'} \bar{\mathbf{\Omega}}_t \bar{\mathbf{g}}_{l,t}^{(r)} = \gamma_{2,l}^{(r)'} \left(\bar{\mathbf{\Sigma}}_{2,l,t}^{(r)} \right)^{-1} \gamma_{2,l}^{(r)} \quad (\text{B.11})$$

$$-2(\mathbf{u}_t - \bar{\mathbf{g}}_{l,t}^{(-r)})' \bar{\mathbf{\Omega}}_t \bar{\mathbf{g}}_{l,t}^{(r)} = -2\bar{\boldsymbol{\mu}}_{2,l,t}^{(r)'} \left(\bar{\mathbf{\Sigma}}_{2,l,t}^{(r)} \right)^{-1} \gamma_{2,l}^{(r)}. \quad (\text{B.12})$$

By Bayes' theorem and plugging eq. (B.11) and eq. (B.12) into eq. (B.8) we get

$$p(\gamma_{2,l}^{(r)} | \boldsymbol{\theta}) = \exp \left(-\frac{1}{2} \left(\gamma_{2,l}^{(r)'} \left((\bar{\mathbf{\Lambda}}_{2,l}^r)^{-1} + \sum_{t \in \mathcal{T}_l} \left(\bar{\mathbf{\Sigma}}_{2,l,t}^{(r)} \right)^{-1} \right) \gamma_{2,l}^{(r)} - 2 \left(\bar{\boldsymbol{\zeta}}_{2,l}^{r'} \left(\bar{\mathbf{\Lambda}}_{2,l}^r \right)^{-1} + \sum_{t \in \mathcal{T}_l} \bar{\boldsymbol{\mu}}_{2,l,t}^{(r)'} \left(\bar{\mathbf{\Sigma}}_{2,l,t}^{(r)} \right)^{-1} \right) \gamma_{2,l}^{(r)} \right),$$

that is the kernel of the desired multivariate normal distribution.

B.5.3 Full conditional distribution of $\gamma_{3,l}^{(r)}$

The full conditional distribution of $\gamma_{3,l}^{(r)}$ is obtained from eqs. (B.6) and (B.8), where

$$\bar{\mathbf{g}}_{l,t}^{(r)'} \bar{\mathbf{\Omega}}_t \bar{\mathbf{g}}_{l,t}^{(r)} = \gamma_{3,l}^{(r)'} \left(\bar{\mathbf{\Sigma}}_{3,l,t}^{(r)} \right)^{-1} \gamma_{3,l}^{(r)} \quad (\text{B.13})$$

$$-2(\mathbf{u}_t - \bar{\mathbf{g}}_{l,t}^{(-r)})' \bar{\mathbf{\Omega}}_t \bar{\mathbf{g}}_{l,t}^{(r)} = -2\bar{\boldsymbol{\mu}}_{3,l,t}^{(r)'} \left(\bar{\mathbf{\Sigma}}_{3,l,t}^{(r)} \right)^{-1} \gamma_{3,l}^{(r)}. \quad (\text{B.14})$$

By Bayes' theorem and plugging eq. (B.13) and eq. (B.14) into eq. (B.8) we get

$$p(\gamma_{3,l}^{(r)} | \boldsymbol{\theta}) = \exp \left(-\frac{1}{2} \left(\gamma_{3,l}^{(r)'} \left((\bar{\mathbf{\Lambda}}_{3,l}^r)^{-1} + \sum_{t \in \mathcal{T}_l} \left(\bar{\mathbf{\Sigma}}_{3,l,t}^{(r)} \right)^{-1} \right) \gamma_{3,l}^{(r)} - 2 \left(\bar{\boldsymbol{\zeta}}_{3,l}^{r'} \left(\bar{\mathbf{\Lambda}}_{3,l}^r \right)^{-1} + \sum_{t \in \mathcal{T}_l} \bar{\boldsymbol{\mu}}_{3,l,t}^{(r)'} \left(\bar{\mathbf{\Sigma}}_{3,l,t}^{(r)} \right)^{-1} \right) \gamma_{3,l}^{(r)} \right).$$

that is the kernel of the desired multivariate normal distribution.

B.5.4 Full conditional distribution of $\gamma_{4,l}^{(r)}$

The full conditional distribution of $\gamma_{4,l}^{(r)}$ is obtained from eqs. (B.3) and (B.8), where

$$\bar{\mathbf{g}}_{l,t}^{(r)'} \bar{\mathbf{\Omega}}_t \bar{\mathbf{g}}_{l,t}^{(r)} = \gamma_{4,l}^{(r)'} \left(\bar{\mathbf{\Sigma}}_{4,l,t}^{(r)} \right)^{-1} \gamma_{4,l}^{(r)} \quad (\text{B.15})$$

$$-2(\mathbf{u}_t - \bar{\mathbf{g}}_{l,t}^{(-r)})' \bar{\mathbf{\Omega}}_t \bar{\mathbf{g}}_{l,t}^{(r)} = -2\bar{\boldsymbol{\mu}}_{4,l,t}^{(r)'} \left(\bar{\mathbf{\Sigma}}_{4,l,t}^{(r)} \right)^{-1} \gamma_{4,l}^{(r)}. \quad (\text{B.16})$$

By Bayes' theorem and plugging eq. (B.15) and eq. (B.16) into eq. (B.8) we get

$$p(\gamma_{4,l}^{(r)} | \boldsymbol{\theta}) = \exp \left(-\frac{1}{2} \left(\gamma_{4,l}^{(r)'} \left((\bar{\mathbf{\Lambda}}_{4,l}^r)^{-1} + \sum_{t \in \mathcal{T}_l} \left(\bar{\mathbf{\Sigma}}_{4,l,t}^{(r)} \right)^{-1} \right) \gamma_{4,l}^{(r)} - 2 \left(\bar{\boldsymbol{\zeta}}_{4,l}^{r'} \left(\bar{\mathbf{\Lambda}}_{4,l}^r \right)^{-1} + \sum_{t \in \mathcal{T}_l} \bar{\boldsymbol{\mu}}_{4,l,t}^{(r)'} \left(\bar{\mathbf{\Sigma}}_{4,l,t}^{(r)} \right)^{-1} \right) \gamma_{4,l}^{(r)} \right),$$

that is the kernel of the desired multivariate normal distribution.

B.6 Full conditional distribution of $\omega_{ijk,t}$

Define $\psi_{ijk,t} = \mathbf{z}'_t \mathbf{g}_{ijk,s_t}$. The posterior full conditional distribution is

$$\begin{aligned}
p(\omega_{ijk,t} | x_{ijk,t}, s_t, \mathcal{G}_{s_t}) &= \sum_{d_{ijk,t} \in \{0,1\}} \int p(\omega_{ijk,t}, d_{ijk,t} | x_{ijk,t}, s_t, \mathcal{G}_{s_t}, \rho_{s_t}) p(\rho_{s_t}) d\rho_{s_t} \\
&= \sum_{d_{ijk,t} \in \{0,1\}} \int \exp(\kappa_{ijk,t}^{(s_t)} \psi_{ijk,t}) \frac{\exp(\psi_{ijk,t} x_{ijk,t} (1 - d_{ijk,t}))}{(1 + \exp(\psi_{ijk,t}))^{1-d_{ijk,t}}} \exp\left(-\frac{\omega_{ijk,t}}{2} \psi_{ijk,t}^2\right) p(\omega_{ijk,t}) p(\rho_{s_t}) d\rho_{s_t} \\
&= \left(1 + \frac{1 + \exp(\psi_{ijk,t})}{\exp(\psi_{ijk,t}/2)}\right) \left(\exp(-\psi_{ijk,t}^2 \omega_{ijk,t}/2) p(\omega_{ijk,t})\right) \\
&\propto \exp(-\psi_{ijk,t}^2 \omega_{ijk,t}/2) p(\omega_{ijk,t}).
\end{aligned}$$

Since $p(\omega_{ijk,t}) \sim PG(1, 0)$, by [43, Theorem 1] the result in eq. (24).

B.7 Full conditional distribution of $d_{ijk,t}$

The posterior full conditional posterior distribution is

$$\begin{aligned}
p(d_{ijk,t} = 1 | \mathcal{X}, \mathbf{s}, \mathcal{G}_{s_t}, \boldsymbol{\rho}_{s_t}) &\propto \rho_{s_t} \delta_{\{0\}}(x_{ijk,t}) \\
p(d_{ijk,t} = 0 | \mathcal{X}, \mathbf{s}, \mathcal{G}_{s_t}, \boldsymbol{\rho}_{s_t}) &\propto (1 - \rho_{s_t}) \frac{\exp((\mathbf{z}'_t \mathbf{g}_{ijk,s_t}) x_{ijk,t})}{1 + \exp(\mathbf{z}'_t \mathbf{g}_{ijk,s_t})},
\end{aligned}$$

which is the discrete distribution in eq. (25), and follows from

$$p(d_{ijk,t} | \mathcal{X}, \mathbf{s}, \mathcal{G}_{s_t}, \boldsymbol{\rho}_{s_t}) \propto (\rho_{s_t} \delta_{\{0\}}(x_{ijk,t}))^{d_{ijk,t}} \left((1 - \rho_{s_t}) \frac{\exp(\mathbf{z}'_t \mathbf{g}_{ijk,s_t}) x_{ijk,t}}{1 + \exp(\mathbf{z}'_t \mathbf{g}_{ijk,s_t})} \right)^{1-d_{ijk,t}}.$$

B.8 Full conditional distribution of ρ_l

The posterior full conditional distribution is

$$\begin{aligned}
p(\rho_l | \mathcal{X}, \mathcal{D}, \mathbf{s}) &\propto \left(\prod_{t \in \mathcal{T}_l} \prod_{i=1}^I \prod_{j=1}^J \prod_{k=1}^K \rho_l^{d_{ijk,t}} (1 - \rho_l)^{1-d_{ijk,t}} \right) \rho_l^{\bar{a}_l^{\rho} - 1} (1 - \rho_l)^{\bar{b}_l^{\rho} - 1} \\
&= \rho_l^{N_l^{\rho} + \bar{a}_l^{\rho} - 1} (1 - \rho_l)^{N_l^{\rho} + \bar{b}_l^{\rho} - 1},
\end{aligned}$$

which is the kernel of the Beta in eq. (32), and we have defined

$$N_1^l = \sum_{t \in \mathcal{T}_l} \sum_{i=1}^I \sum_{j=1}^J \sum_{k=1}^K \mathbb{1}_{\{1\}}(d_{ijk,t}), \quad N_0^l = \sum_{t \in \mathcal{T}_l} \sum_{i=1}^I \sum_{j=1}^J \sum_{k=1}^K \mathbb{1}_{\{0\}}(d_{ijk,t}).$$

B.9 Full conditional distribution of ξ_l

The posterior full conditional distribution of each row l is

$$\begin{aligned} p(\xi_l | \mathbf{s}) &\propto \left(\prod_{k=1}^L \xi_{l,k}^{\bar{c}_k - 1} \right) \left(\prod_{g=1}^L \prod_{k=1}^L \xi_{g,k}^{N_{g,k}(\mathbf{s})} \right) \\ &\propto \prod_{k=1}^L \xi_{l,k}^{\bar{c}_k + N_{l,k}(\mathbf{s}) - 1}, \end{aligned}$$

which is the kernel of the Dirichlet in eq. (33), and $N_{i,j}(\mathbf{s}) = \sum_t \zeta_{t-1,i} \zeta_{t,j}$.

B.10 Full conditional distribution of s_t

We update the whole path \mathbf{s} from the posterior full joint conditional distribution via the Forward Filtering Backward Sampling algorithm (FFBS, see [22]). It is based on the factorisation of the full joint conditional distribution as the product of the entries of the transition matrix Ξ and the filtered probabilities $p(\mathbf{s}_t | \mathcal{X}_1, \dots, \mathcal{X}_t, \mathcal{G}, \boldsymbol{\rho}, \Xi)$. The full joint conditional distribution:

$$p(\mathbf{s} | \mathcal{X}, \mathcal{G}, \boldsymbol{\rho}, \Xi) \propto p(\mathbf{s} | \Xi) \prod_{i=1}^I \prod_{j=i}^J \prod_{k=1}^K p(x_{ijk,t} | s_t = l, \rho_l, \mathcal{G}_l).$$

C Computational Details for the Pooled Model

Let \mathcal{H} be a tensor of size $(I \times J \times K \times Q \times Q)$ with entries defined by

$$\mathcal{H}_{ijkqp} = \begin{cases} 1 & \text{if } q = p \\ 0 & \text{if } q \neq p \end{cases}$$

for each ijk . If $\mathbf{g}_{ijk,l} = \mathbf{g}_l \in \mathbb{R}^Q$ for each ijk and regime l , then we have the representation $\mathcal{G}_l = \mathcal{H} \times_5 \mathbf{g}_l$. In the pooled model we are assuming that the coefficient tensor in each regime l satisfies $\mathcal{G}_{ijkq,l} = \mathbf{g}_{q,l}$. We assume the following prior distributions

$$\mathbf{g}_l | \tau, w_l \sim \mathcal{N}_Q(\bar{\boldsymbol{\zeta}}_l, \tau w_l \mathbf{I}_Q), \quad w_l | \lambda_l \sim \text{Exp}(\lambda_l^2/2), \quad \lambda_l \sim \mathcal{G}a(\bar{a}_l^\lambda, \bar{b}_l^\lambda), \quad \tau \sim \mathcal{G}a(\bar{a}^\tau, \bar{b}^\tau).$$

The complete data likelihood thus becomes

$$L(\mathcal{X} | \boldsymbol{\theta}) \propto \prod_{t \in \mathcal{T}_l} \prod_{i=1}^I \prod_{j=1}^J \prod_{k=1}^K \exp \left(-\frac{\omega_{ijk,t} (\mathbf{z}'_t \mathbf{g}_l)^2}{2} + \kappa_{ijk,t} (\mathbf{z}'_t \mathbf{g}_l) \right).$$

This yields the posterior distribution for \mathbf{g}_l

$$\begin{aligned} p(\mathbf{g}_l | \boldsymbol{\Omega}_t, \tau, w_l) &\propto \exp \left(-\frac{1}{2} \sum_{t \in \mathcal{T}_l} \sum_{i,j,k} \mathbf{g}'_l \mathbf{z}_t \omega_{ijk,t} \mathbf{z}'_t \mathbf{g}_l - 2 \mathbf{z}'_t \mathbf{g}_l \kappa_{ijk,t} \right) \exp \left(-\frac{1}{2} \frac{(\mathbf{g}_l - \bar{\boldsymbol{\zeta}}_l)' (\mathbf{g}_l - \bar{\boldsymbol{\zeta}}_l)}{\tau w_l} \right) \\ &= \exp \left(-\frac{1}{2} \left(\mathbf{g}'_l \left(\frac{1}{\tau w_l} + \sum_{t \in \mathcal{T}_l} \sum_{i,j,k} \mathbf{z}_t \omega_{ijk,t} \mathbf{z}'_t \right) \mathbf{g}'_l - 2 \left(\frac{\bar{\boldsymbol{\zeta}}'_l}{\tau w_l} + \sum_{t \in \mathcal{T}_l} \sum_{i,j,k} \kappa_{ijk,t} \mathbf{z}'_t \right) \mathbf{g}_l \right) \right), \end{aligned}$$

which is the kernel of a Normal distribution. The posterior distribution of τ is

$$\begin{aligned} p(\tau | \mathbf{g}, \mathbf{w}) &\propto \tau^{\bar{a}^\tau - 1} \exp(-\bar{b}^\tau \tau) \prod_{l=1}^L \exp \left(-\frac{(\mathbf{g}_l - \bar{\boldsymbol{\zeta}}_l)' (\mathbf{g}_l - \bar{\boldsymbol{\zeta}}_l)}{2\tau w_l} \right) \\ &= \tau^{\bar{a}^\tau - 1} \exp \left(-\frac{1}{2} \left(2\bar{b}^\tau \tau + \sum_{l=1}^L \frac{(\mathbf{g}_l - \bar{\boldsymbol{\zeta}}_l)' (\mathbf{g}_l - \bar{\boldsymbol{\zeta}}_l)}{w_l} \frac{1}{\tau} \right) \right), \end{aligned}$$

which is the kernel of a GiG distribution. The posterior distribution of w_l is

$$\begin{aligned} p(w_l | g_l, \tau, \lambda_l) &\propto \exp \left(-\frac{\lambda_l^2}{2} w_l \right) \exp \left(-\frac{(\mathbf{g}_l - \bar{\boldsymbol{\zeta}}_l)' (\mathbf{g}_l - \bar{\boldsymbol{\zeta}}_l)}{2\tau w_l} \right) \\ &= \exp \left(-\frac{1}{2} \left(\lambda_l^2 w_l + \frac{(\mathbf{g}_l - \bar{\boldsymbol{\zeta}}_l)' (\mathbf{g}_l - \bar{\boldsymbol{\zeta}}_l)}{\tau} \frac{1}{w_l} \right) \right), \end{aligned}$$

which is the kernel of a GiG distribution. The posterior distribution of λ_l (integrating out w_l) is again a GiG obtained from

$$\begin{aligned} p(\lambda_l | \tau, \mathbf{g}_l) &\propto \lambda_l^{\bar{a}_l^\lambda - 1} \exp(-\bar{b}_l^\lambda \lambda_l) \frac{\sqrt{\tau}}{2\lambda_l} \exp \left(-\frac{\|\mathbf{g}_l\|_1 \sqrt{\tau}}{\lambda_l} \right) \\ &\propto \lambda_l^{\bar{a}_l^\lambda - 2} \exp \left(-\frac{1}{2} \left(2\bar{b}_l^\lambda \lambda_l + \|\mathbf{g}_l\|_1 \sqrt{\tau} / \lambda_l \right) \right). \end{aligned}$$